



Characterization of doxorubicin binding site and drug induced alteration in the functionally important structural state of oxyhemoglobin

Shahper N. Khan^a, Barira Islam^a, Ragothaman Yennamalli^b, Qamar Zia^a, Naidu Subbarao^b, Asad U. Khan^{a,*}

^a Interdisciplinary Biotechnology Unit, Aligarh Muslim University, Aligarh-202002, India

^b Centre for Computational Biology and Bioinformatics, School of Information Technology, Jawaharlal Nehru University, New Delhi-110067, India

ARTICLE INFO

Article history:

Received 15 May 2008

Received in revised form 12 August 2008

Accepted 21 August 2008

Available online 4 September 2008

Keywords:

Hemoglobin

Doxorubicin

Binding mode

Fluorescence resonance energy transfer

(FRET)

Molecular docking

ABSTRACT

Doxorubicin (DOX) binding to hemoglobin (Hb) was studied to investigate the drug induced protein dysfunction. The features of anti-tumor drug doxorubicin induced structural perturbation of human Hb were studied by circular dichroism (CD). The mechanism of DOX–Hb binding was elucidated by steady-state and synchronous fluorescence spectroscopy. The Stern–Volmer analysis indicated that the binding of Hb to DOX is characterized by more than one high affinity binding site with the association constants of the order of 10^5 . Hydrophobic probe ANS was employed to elucidate the drug binding site. Binding mode expounded by thermodynamic parameters implied the role of hydrogen bonding, electrostatic and hydrophobic interaction in stabilizing the complex. The molecular distance between donor (Hb) and acceptor (DOX) was calculated according to Förster's theory of energy transfer. Fourier transform infrared (FT-IR) spectroscopy provides an insight to the changes occurring in protein on DOX binding. Treatment of Hb with DOX resulted in a dose dependent fragmentation of protein. The quantitative analysis revealed the release of acid soluble amino groups from the photoexcited Hb–DOX mixture. The free radical mediated degradation was suggested by its rescue on mannitol and superoxide dismutase (SOD) appliance. The loss of protein band further corroborates the concentration dependent Hb fragmentation. The molecular modeling complies with the thermodynamic data of forces involved in DOX binding and depicts its interaction in the proximity of oxygen binding pocket of Hb. Thus, this study enriches our understanding of the interaction dynamics of anticancer drugs to the physiologically important protein Hb.

© 2008 Elsevier B.V. All rights reserved.

1. Introduction

Hemoglobin (Hb) is the iron containing oxygen transport metalloprotein in the red blood cells. It also aids, both directly and indirectly, the transport of carbon dioxide and regulates the pH of blood [1]. It is a concatenation of heme and globin. It comprises two α - and two β -chains assembled to form symmetrical ($\alpha\beta$) dimers forming an essential quaternary structure. Quaternary organization and the associated subunit interaction property of tetrameric Hb confers it to have the regulatory property when small ligands such as metabolites or drugs bind to it and modulate the functional activity of this important protein. The Hb exists in two functionally important isomeric forms: the R form (oxygen/ligand bound state) and the T form (Deoxy state) [2,3], which assist coordination between the upload and release of oxygen. Doxorubicin (DOX)

is an effective agent in the treatment of breast cancer, malignant lymphomas, soft tissue sarcoma and various neoplastic diseases. This anthracycline antibiotic (Fig. 1) has a water soluble basic amino sugar, daunosamine that is linked glycosidically to carbon 7 of a four-ringed water insoluble aglycone known as doxorubicinone. This aglycone is a substituted naphthacene quinone with a methoxy group at the 4-position and a hydroxyl group plus a hydroxyacetyl group at carbon 9 [4]. DOX form covalent adducts with DNA exclusively at GpC sequences leading to impairment of topoisomerase II activity. This interaction impedes cellular functions that involve DNA (*i.e.* replication and transcription) by forming interstrand cross-links. Although DOX is a very effective anti-tumor drug, its usefulness is limited due to its various toxicities [5,6]. Redox cycling of DOX has been shown to initiate free radical reactions with cell constituents. Free radical induced scission of DNA appears to be important for the anti-tumor activity of the drug [7,8] and lipid peroxidation could be the cause of its cardiotoxicity [9]. DOX has been shown to oxidize Hb [10] and to produce superoxide in red cells [11]. This may result in hemolysis, particularly in glucose 6-phosphate dehydrogenase-deficient red cells [12].

* Corresponding author. Tel.: +91 571 2723088; fax: +91 571 2721776.

E-mail addresses: asad.k@rediffmail.com, asadukhan72@gmail.com (A.U. Khan).

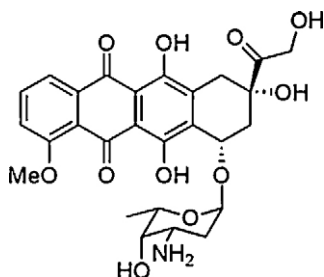


Fig. 1. Chemical structure of doxorubicin (DOX), an anthracycline antibiotic.

It has been suggested that on reduction DOX reacts directly with oxyHb [13]. It had been previously reported that anthracyclines binds to Hb [14,15] but the binding mode and binding site have not yet been well characterized. The role of iron in DOX metabolism is of critical importance [16,17]. It is the DOX+ iron (III) complex that undergoes self-reduction to an iron (II) complex and forms a semiquinone free radical, which reduces oxygen or hydrogen peroxide to yield the hydroxyl free radical [8]. Therefore, the important biological element that facilitates the development of various toxicities is the availability of iron. Importantly, the total iron content in the body of normal adults is approximately 3–5 g and of which 1.5–3 g, more than 50% of the total iron content is estimated to be associated with Hb. Hence, understanding the role that Hb plays in disposition of DOX or its interaction with the drug at the cellular level may have important clinical implications. The purpose of this study was to investigate the *in vitro* interaction of DOX with Hb. The direct interaction of this protein with drugs may also affect its functionally important structural conformation or might interfere with the vital oxygen transport process. The intended goal was to identify the most relevant detail about this drug–protein interaction. The interaction was systematically investigated by sensitive optical spectroscopy [18,19], biochemical estimations and molecular modeling studies.

2. Experimental

2.1. Materials

Human hemoglobin (Hb), superoxide dismutase (SOD), 1-anilinonaphthalene-8-sulfonate (ANS) and trinitrobenzene sulphonic acid (TNBS) were purchased from Sigma Chemical Company, St. Louis, USA. Doxorubicin (DOX) also known as adriamycin was purchased from Ranbaxy, India. All other materials were of analytical reagent grade. The protein concentration was determined spectrophotometrically. The white light 20 W/m² of photosynthetically active radiation (PAR) emitted from a Philips 40 W fluorescent lamp with PAR TLD tubes was used for light exposure. All samples were exposed to luminous radiation in borosilicate tubes. The light intensity was measured with a PMA 2100 radiometer (Solar light, Philadelphia, USA).

2.2. Purification of Hb

The higher molecular weight aggregates associated with commercial preparations of Hb were removed by size exclusion chromatography on a G-100 Sephadex column (120 cm × 1 cm) pre-equilibrated with 60 mM phosphate buffer, pH 7.4. Fractions of 1 ml were collected at a flow rate of 10 ml h⁻¹ and the purity was ascertained by SDS-PAGE. Protein concentration of the Hb fractions was determined spectrophotometrically at 398 nm using an extinction coefficient of $1.56 \times 10^5 \text{ M}^{-1} \text{ cm}^{-1}$ [20]. The solutions of Hb were prepared in 0.1 M phosphate buffer at pH 7.4 to obtain mainly R form

of protein [3], which was further characterized by its fluorescence properties.

2.3. Circular dichroism (CD) measurements

The CD measurements were made on a JASCO-J-720 spectropolarimeter (Tokyo, Japan) and calibrated with d-10-camphor sulfonic acid. Dry nitrogen gas was purged before and during the course of measurements. The CD measurements of Hb in absence and presence of DOX were made in the range of 200–250 nm using a 0.1 cm cell at 0.2 nm intervals with three scans averaged for each CD spectra. The samples for CD were prepared with the fixed concentration of Hb (3 μM) and varied drug concentration resulting in equal volumes. The molar ratio of Hb to drug concentration was 1:0, 1:2 and 1:4 for CD spectra.

2.4. Steady-state fluorescence

Fluorescence measurements were performed on a spectrofluorimeter Model RF-5301PC (Shimadzu, Japan) equipped with a 150 W Xenon lamp and a slit width of 5 nm. A 1.0 cm quartz cell was used for measurements. The working concentration of Hb used was 3 μM so as to prevent quenching of Trp fluorescence by the neighboring Heme group [21] and increasing amounts of drug stock solution (200 μM) was added starting from 1:1 to 1:10. Fluorescence spectra were recorded at 298, 306 and 310 K in the range of 300–500 nm upon excitation at 280 nm.

2.5. Synchronous fluorescence spectroscopy

Synchronous fluorescence spectra of Hb in the absence and presence of increasing amount of DOX ($0\text{--}27 \times 10^{-6} \text{ mol l}^{-1}$) were recorded λ_{ex} : 300–360 nm and a constant difference of $\Delta\lambda = 30 \text{ nm}$ and 60 nm was maintained.

2.6. Energy transfer between DOX and Hb

The absorption spectrum of DOX (3 μM) was recorded in the range of 300–400 nm. The emission spectrum of Hb (3 μM) was also recorded in the range of 300–400 nm on excitation at 295 nm. The overlap of the UV absorption spectrum of DOX with the fluorescence emission spectrum of protein was used to calculate the energy transfer as per Förster's theory [22].

2.7. Hydrophobic probe displacement

Experiments were also carried out in the presence of hydrophobic probe, ANS. In the first set of experiments, interaction of drug and ANS with Hb was studied under identical conditions. Hb concentration was kept fixed at 3 μM and ANS/drug concentration was varied from 3 to 30 μM. Fluorescence of Hb was recorded at 334 nm after excitation at 280 nm. In the second set of experiments, increasing amount of drug (3–30 μM) was added to equimolar Hb–ANS mixture (3 μM each) and the fluorescence of ANS was recorded at 470 nm after excitation at 370 nm. The concentration of Hb:ANS mixture was kept fixed by adding the same volume of Hb–ANS mixture as of drug.

2.8. FT-IR spectroscopic measurements

Infrared spectra of protein solution were recorded on a Interspec 2020 FT-IR spectrophotometer (DTGS detector and KBr beam splitter) via the attenuated total reflection (ATR) method with resolution of 4 cm^{-1} and 60 scans. Spectra processing procedures: spectra of

sample solution and buffer solution were collected at the same condition. Then, subtract the absorbance of buffer solution from the spectra of sample solution to get the FT-IR spectra of proteins. The subtraction criterion was that the original spectrum of protein solution between 2200 and 1800 cm^{-1} was not depicting any significant signal in this region [23].

2.9. Estimation of protein degradation

Degradation of protein was assessed by measuring the TCA soluble amino groups with TNBS reagent according to the method of Snyder and Sobocinski [24]. A typical reaction mixture containing Hb (100 μM), varying concentrations of DOX (0–1000 μM) was exposed to white light for 3 h for dose dependent and one concentration of drug with varying time incubation for time dependent effect of drug on protein at 310 K. The reactions were carried out in the presence of PMSF (10 $\mu\text{g}/100\text{ ml}$) to minimize proteolytic degradation. Reactions were stopped with the addition of 100 μM EDTA followed by precipitation with 5% (w/v) Trichloroacetic acid solution. The supernatant was obtained after centrifugation at 2500 rpm for 30 min and acid soluble amino groups were quantitated using the calibration curve of glycine. The absorbance was read at 335 nm and plotted as a function of DOX concentration and time of exposure to white light. Inhibition of protein fragmentation was also monitored in the presence of SOD, ethanol, DMSO and mannitol as free radical scavengers.

2.10. SDS-PAGE

Hb was incubated with DOX (1:2, 1:4 and 1:8 molar ratio of Hb:DOX) exposed to white light for 8 h at 310 K. The reaction mixture was centrifuged at 2500 rpm. The protein concentration was measured spectrophotometrically and gel was loaded with 10 μg per well. The SDS-PAGE and commasie blue staining were performed according to Laemmli [25].

2.11. Molecular modeling study

Molecular docking simulations of Hb–DOX were performed with GOLDv3.1.1 program [26]. The crystal structure of Hb (PDB Id: 1HHO) was downloaded from the Brookhaven Protein Data Bank (<http://www.rcsb.org/pdb>). The two-dimensional (2D) structure of DOX was downloaded from Pubchem (<http://www.pubchem.ncbi.nlm.nih.gov>). 2D to three-dimensional (3D) conversion was done with CORINA [27]. The structure of Hb was protonated in Insight II (<http://www.accelrys.com>). Genetic algorithm implemented in GOLDv3.1.1 was applied to calculate the possible conformations of the DOX that binds to the protein. The genetic algorithm parameters used are: Population size, 100; Number of Islands, 5; Niche size, 2; Selection pressure, 1.1; Migrate, 2; Number of operators, 100,000; Mutate, 95; Crossover, 95. During the docking process, a maximum of 10 different conformations was considered for the drug. The conformer with the lowest binding free energy was used for further analysis and a fitness score is calculated. The binding energy for different conformation was predicted using X-Score [28]. The residues that are making hydrogen bonding and hydrophobic interactions were calculated using Getneares, a tool available with DOCKv5.1.1 [29].

3. Result and discussion

3.1. Circular dichroism (CD) analysis

CD spectroscopy was used to investigate alterations in the secondary structure of Hb after addition of DOX. In this experiment,

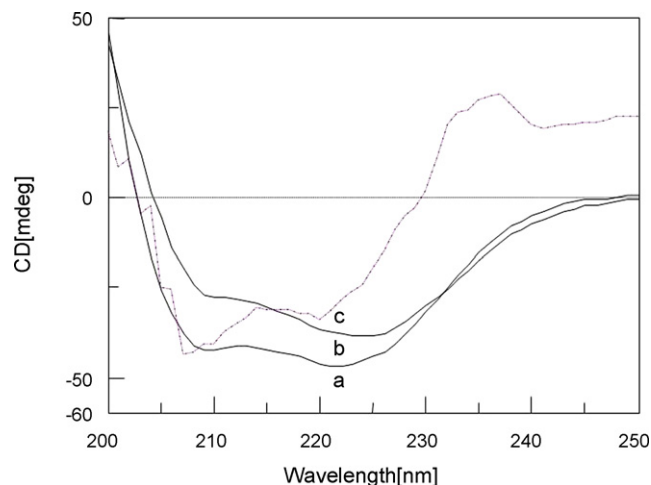


Fig. 2. The far UV-CD spectra of Hb native (a), native+6 μM DOX (b), and native+12 μM DOX (c).

the molar ratios of 1:0, 1:2 and 1:4 for Hb:DOX were used for the CD measurements. The CD spectra of Hb in the absence (line a) and presence (lines b and c) of DOX are shown in Fig. 2. The CD results were expressed in terms of mean residue ellipticity (MRE) in $\text{deg cm}^2 \text{ dmol}^{-1}$ (Table 1), according to the following equation:

$$\text{MRE} = \frac{\text{observed CD (mdeg)}}{C_p n l \times 10} \quad (1)$$

where C_p is the molar concentration of the protein, n is the number of amino acid residues and l is the path length. The α -helical contents of free and combined Hb were calculated from MRE values at 208 nm using the equation [30]:

$$\alpha\text{-helix (\%)} = \frac{-\text{MRE}_{208} - 4000 \times 100}{33,000 - 4000} \quad (2)$$

where MRE_{208} is the observed MRE value at 208 nm, 4000 is the MRE of the β -form and random coil conformation cross at 208 nm and 33,000 is the MRE value of a pure α -helix at 208 nm. The CD spectra of Hb exhibited two negative bands in the UV region at 208 and 222 nm (Fig. 2), characteristic of a α -helical structure of protein [31]. Addition of DOX resulted in the reduction in ellipticity (curves b and c), which is accompanied by the decrease in α -helix by 28.01%. This illustrates the destabilization of the native secondary structure of Hb on DOX binding, which implicates the interference of the drug with the secondary structure supportive bonds/interaction forces and results in structural transition (Table 1). Resulted drastic variation in the protein helical content can be inferred by the significant change in the spectral pattern. It is important to quote that saturable binding of some ligands to Hb induce alterations in the structure and function of this protein. However, competitive binding displayed by different ligands may result from allosteric effects, whereby binding of ligand A at a certain site causes a

Table 1
Circular dichroism (CD) derived alterations in the secondary structure of Hb on DOX interaction

Hb:DOX (molar ratio)	MRE ₂₂₂ ^a	% α -Helix ^b	% β sheet and random coils structures
1:0	−21,153	62.10	37.90
1:2	−19,384	56.20	47.80
1:4	−15,885	44.70	55.30

^a MRE in $\text{deg cm}^2 \text{ dmol}^{-1}$.

^b Average values for three independent observations and the S.D. was 0.3–0.7%.

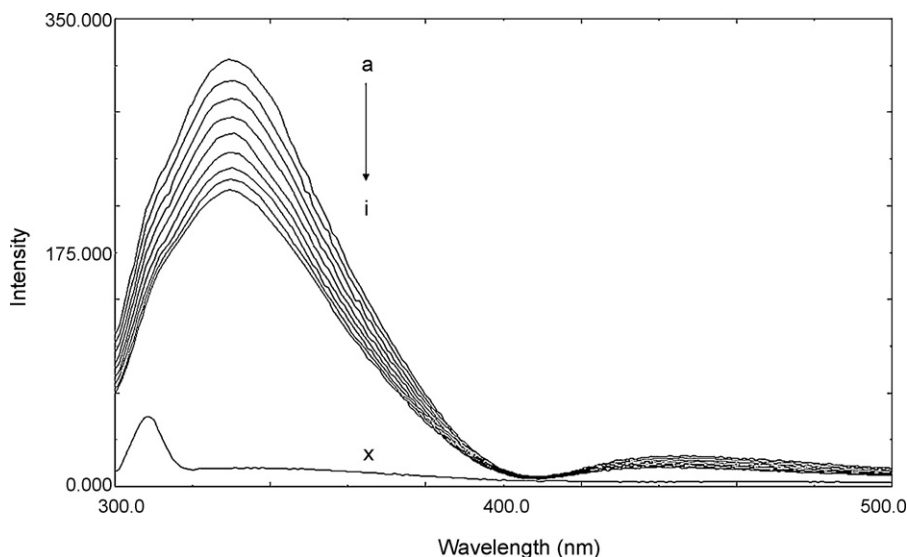


Fig. 3. Fluorescence emission spectra of Hb concentration 3 μM (a) in phosphate buffer, pH 7.4, temperature 298 K in the absence and presence of DOX after exciting it at 280 nm. The DOX concentration was 3 μM (b), 6 μM (c), 9 μM (d), 12 μM (e), 15 μM (f), 18 μM (g), 21 μM (h), 24 μM (i) and 3 μM DOX alone (x).

conformational change in the protein so that binding of ligand B at a different site is altered [32].

3.2. Binding property of the DOX to Hb

Fluorescence spectroscopy was used to measure the change in the tertiary structure of protein induced by different concentrations of DOX. The effect of drug on Hb fluorescence intensity is shown in Fig. 3. The addition of DOX caused a gradual decrease in the fluorescence emission intensity of Hb with a conspicuous change in the emission spectra. It can be seen that a higher excess of DOX led to more effective quenching of the chromophore molecule fluorescence. The quenching of the Hb fluorescence clearly indicated that the binding of the drug to Hb changed the microenvironment of fluorophores and thereby its tertiary structure.

3.2.1. Analysis of binding

To further elaborate the fluorescence quenching mechanism the Stern–Volmer equation was used for data analysis:

$$\frac{F_0}{F} = 1 + K_{SV}[Q] \quad (3)$$

where F_0 and F are the steady-state fluorescence intensities in the absence and presence of quencher, respectively, K_{SV} is the Stern–Volmer quenching constant and $[Q]$ is the concentration of quencher (DOX). However, the Stern–Volmer curve showed upward curvature toward y-axis at higher drug concentrations (Fig. 4). The procedure of quenching was further confirmed from the values of bimolecular quenching rate constants, K_q , which are evaluated using the equation:

$$K_q = \frac{K_{SV}}{\tau_0} \quad (4)$$

where τ_0 is the lifetime of protein without the quencher. The average value of fluorescence lifetime used was about 10^{-8} [33]. The bimolecular quenching rate constants were of the order of $10^{12} \text{ l mol}^{-1} \text{ s}^{-1}$. This was greater than the maximum limiting diffusion constant K_{dif} of the biomolecule ($K_{dif} = 2.0 \times 10^{10} \text{ l mol}^{-1} \text{ s}^{-1}$) [34] suggesting the static type quenching procedure in complex formation. The procedure of quenching was further confirmed by studying the temperature dependence pattern of quenching parameters, which can differentiate between the dynamic and

static quenching. The K_{SV} values decrease with an increase in temperature for static quenching and the reverse will be observed for dynamic quenching. The trend in this study (Table 2) indicates that the probable quenching mechanism of Hb fluorescence by DOX is a static type. When ligand molecules bind independently to a set of equivalent sites on a macromolecule, the equilibrium between free and bound molecules is given by the equation [35]:

$$\log \left[\frac{F_0 - F}{F} \right] = \log K + n \log [Q] \quad (5)$$

where K and n are the binding constant and the number of binding sites, respectively. Thus, a plot of $\log(F_0 - F)/F$ versus $\log[Q]$ can be used to determine K as well as n (Table 2). The values of K suggested that the binding constant decreased with an increase in temperature, resulting in the destabilization of the DOX–Hb complex. Meanwhile, from the data of n it may be inferred that there is more than one (≈ 2) site of binding for DOX. This is understood as Hb comprises of $\alpha_2\beta_2$ dimers (tetramer), hence, the interaction behavior with a monomer is also expected with the other monomer of the dimer.

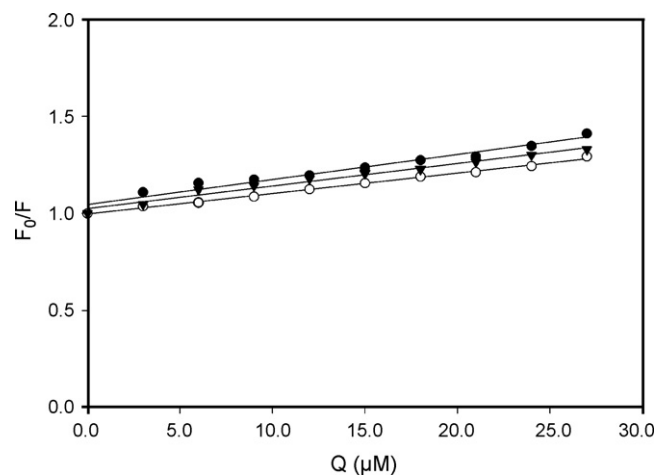


Fig. 4. Stern–Volmer plot for the binding of DOX with Hb at 298 K (●), 306 K (▼) and 310 K (○).

Table 2
Quenching and binding parameters for Hb–DOX interaction

T (K)	K_{SV} ($\times 10^4$ l mol $^{-1}$)	K_q ($\times 10^{12}$ l mol $^{-1}$ s $^{-1}$)	R^2	K ($\times 10^5$ mol $^{-1}$)	n
298	1.28 \pm 0.04	1.28 \pm 0.04	0.989	5.64 \pm 0.16	1.81
306	1.15 \pm 0.05	1.15 \pm 0.05	0.997	5.01 \pm 0.12	1.78
310	1.05 \pm 0.02	1.05 \pm 0.02	0.983	4.75 \pm 0.15	1.75

3.3. Conformation ascribed synchronous fluorescence

Synchronous fluorescence of Hb was studied to evaluate the change in the environment of tyrosine and tryptophan residues as a result of DOX binding. Synchronous mode of fluorescence spectroscopy introduced by Lloyd [36] was applied to infer the conformational changes of the protein due to this binding reaction. Simultaneous scanning of excitation and the emission monochromators with fixed wavelength difference between them was set. According to Miller [37] the characteristic information of tyrosine and tryptophan residue is obtained when $\Delta\lambda$ difference is maintained at 30 and 60 nm, respectively. Fig. 5 shows the effect of addition of DOX on the synchronous fluorescence spectrum of Hb when $\Delta\lambda$ were stabilized at 30 and 60 nm. The addition of the drug shows a slight shift in the emission peak for tyrosine (Fig. 5, panel A). This implicates the change in the environment of tyrosine mainly 140, 42 (of α -chain) and 35 (of β -subunit) present at $\alpha\beta$ interface. The synchronous fluorescence spectra for tryptophan show a red shift (Fig. 5, panel B). The intrinsic fluorescence of Hb primarily originates from the Trp β 37 as reported by Alpert et al. [21]. Hence, the fluorescence studied here is mainly attributed to Trp β 37 present at $\alpha\beta$ interface. An X-ray study [38] pointed out that Tyr α 42 and Trp β 37 are the part of switch region and flexible joint region, respectively, which are responsible for the stabilization of Hb quaternary structure. The changes in these regions suggest the destabilization of protein quaternary structure. However, the red shift in λ_{max} also suggests the conformational relaxation and unfolding of Hb on DOX binding. Hb is the carrier of oxygen, binding of DOX could affectively hinder the physiological functions of Hb by opening its structural state, which is of vital importance in case of structure specific binders as in case of Hb–oxygen binding.

3.4. Fluorescence resonance energy transfer

In the light of published literature, the synchronous study suggested the binding of DOX in the vicinity of Trp β 37, which is the part of flexible joint region in Hb and is involved in the stabilization of its quaternary structure. Hence, the proximity between the protein residue (Trp β 37) and the bound DOX (acceptor) has been predicted using fluorescence resonance energy transfer (FRET). The extent of spectral overlaps determines the extent of energy transfer. Generally, FRET occurs whenever the emission spectrum of a fluorophore (donor) overlaps with the absorption spectrum of another molecule (acceptor). The overlap of the UV absorption spectrum of DOX with the fluorescence emission spectra of Hb is shown in Fig. 6. The good extent of overlap suggests the high degree of energy transfer. The distance between the donor and acceptor can be calculated according to Förster's theory of dipole–dipole energy transfer [22]. The efficiency, E can be calculated using the equation:

$$E = \frac{1 - F}{F_0} = \frac{R_0^6}{R_0^6 + r^6} \quad (6)$$

where F and F_0 are the fluorescence intensities of Hb in the presence and absence of DOX, r is the distance between acceptor and donor and R_0 is the critical distance when the transfer efficiency is 50%.

$$R_0^6 = 8.8 \times 10^{-25} (k^2 \eta^{-4} \Phi J) \quad (7)$$

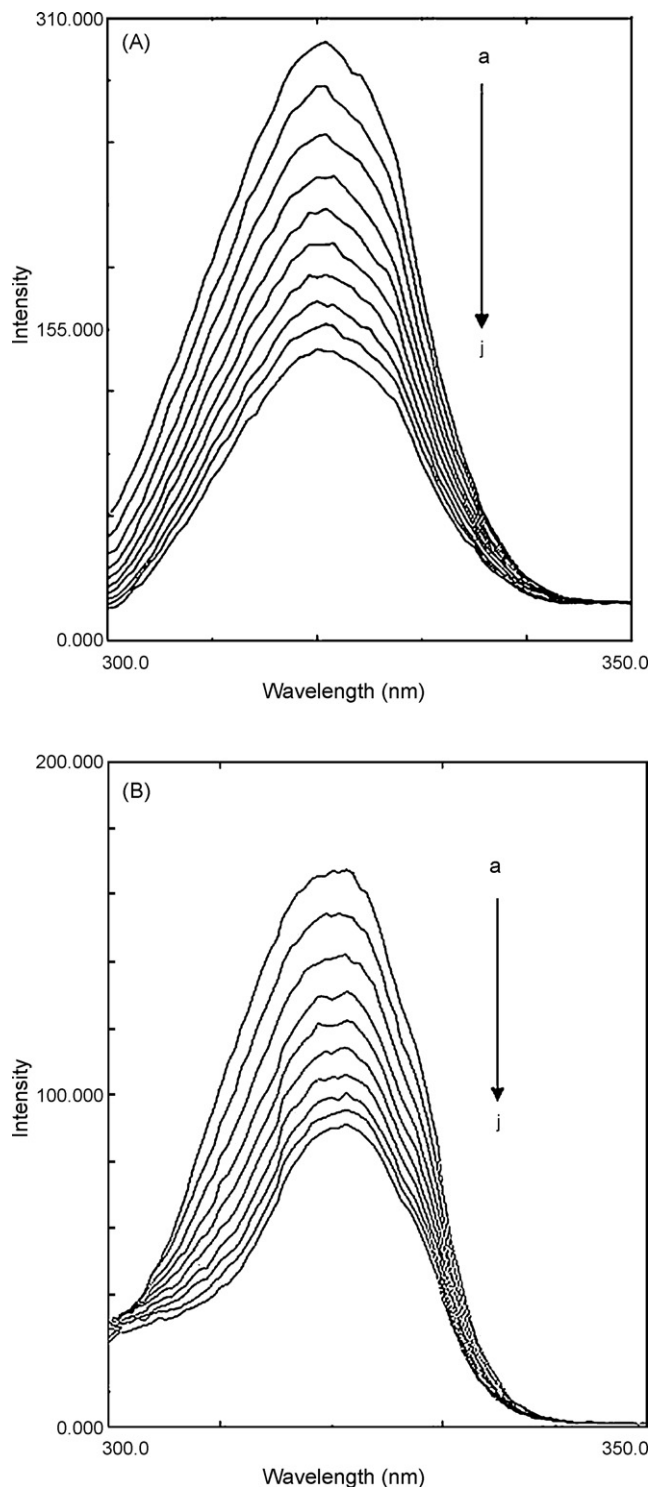


Fig. 5. Synchronous fluorescence spectra of Hb (3 μ M) (A) tyrosine, $\Delta\lambda = 30$ nm and (B) tryptophan, $\Delta\lambda = 60$ nm in the absence and presence of increasing concentration of DOX, i.e. 0 μ M (a), 3 μ M (b), 6 μ M (c), 9 μ M (d), 12 μ M (e), 15 μ M (f), 18 μ M (g), 21 μ M (h), 24 μ M (i) and 27 μ M (j).

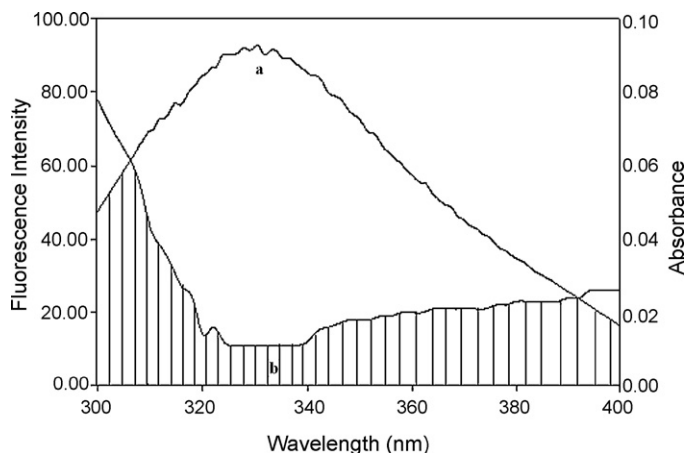


Fig. 6. The overlap of the fluorescence spectrum of Hb (a) and the absorbance spectrum of DOX (b); $[c(\text{Hb})]/c(\text{DOX}) = 1:1$.

where k^2 is the spatial orientation factor of the dipole, η is the refractive index of the medium, Φ is the fluorescence quantum yield of the donor and J is the overlap integral of the fluorescence emission spectrum of the donor and the absorption spectrum of the acceptor. J is approximated by the given equation:

$$J = \frac{\sum F(\lambda)\varepsilon(\lambda)\lambda^4\Delta\lambda}{\sum F(\lambda)\Delta\lambda} \quad (8)$$

where $F(\lambda)$ is the fluorescence intensity of the fluorescent donor of wavelength, λ and $\varepsilon(\lambda)$ is the molar absorption coefficient of the acceptor at wavelength, λ . In the present case, $k^2 = 2/3$, $\eta = 1.36$ and $\Phi = 0.062$ for Hb [39]. From Eqs. (6)–(8), we were able to calculate that $J = 8.96 \times 10^{-15} \text{ cm}^3 \text{ l mol}^{-1}$, $R_0 = 1.99 \text{ nm}$, $E = 0.24$ and $r = 2.41 \text{ nm}$ for Hb. The donor-to-acceptor distance, $r < 8 \text{ nm}$ [39,40] is in accord with Förster's non-radiative energy transfer with high probability and since, r was greater than R_0 in this study suggested that DOX could strongly quench the intrinsic fluorescence of Hb by static quenching mechanism [35].

3.5. Hydrophobic probe ANS

In order to allocate the DOX binding region on Hb, the quenching of protein fluorescence by drug and hydrophobic probe, ANS was determined under identical conditions. Both drugs and ANS quench the fluorescence of Hb. However, the extent of quenching by drugs was much less as compared to ANS. The relative fluorescence intensity (F/F_0 , where F and F_0 are the fluorescence intensity of Hb in the presence and absence of quencher, ANS/drug) versus quencher concentration plots are shown in Fig. 7. In another set of experiments, ANS fluorescence was measured. Relative fluorescence intensity (F/F_0 , where F and F_0 are the fluorescence intensity of ANS in Hb-ANS system, in the presence and absence of drug) has been plotted against the concentration of drug in Fig. 7. The drug when added to Hb-ANS system can compete with ANS for hydrophobic sites on the surface. In that case it would displace ANS from its binding site and the fluorescence intensity should decrease. This happens with DOX binding. However, approx. 45% displacement suggests the presence of multiple binding sites for ANS on Hb molecule [41]. From this study we concluded that hydrophobic patches are the major sites for DOX binding on Hb. Similar findings have also been reported by Seedher et al. [42] for the binding of trifluoperazine dihydrochloride with serum albumin.

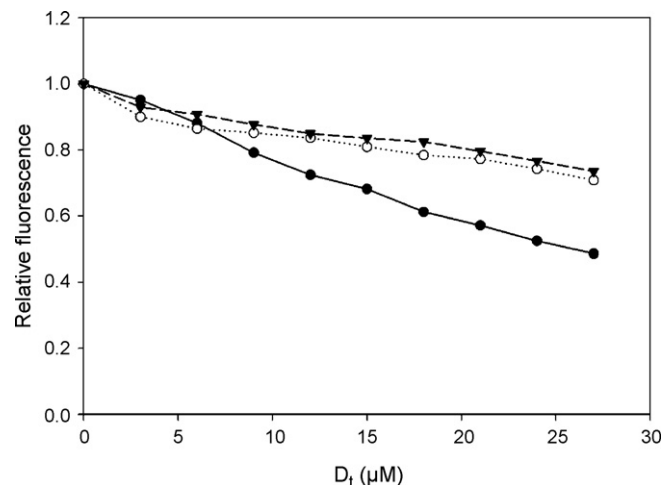


Fig. 7. Fluorescence quenching pattern of Hb and Hb-ANS system. Binding isotherm of DOX (\blacktriangledown) and ANS (\circ) induced quenching of Hb fluorescence and quenching of Hb-ANS system fluorescence by DOX (\bullet).

3.6. Binding mode

Considering the dependence of binding constant on temperature, a thermodynamic process was considered to be responsible for this interaction. Therefore, the thermodynamic parameters dependent on temperatures were analyzed in order to further characterize the acting forces between DOX-Hb complex. The acting forces between a small molecule and macromolecule mainly include hydrogen bonds, van der Waals forces, electrostatic forces and hydrophobic interaction forces. The thermodynamic parameters, enthalpy change (ΔH°), entropy change (ΔS°) and free energy change (ΔG°) are the main evidences to determine the binding mode [43,44]. The thermodynamic parameters were evaluated using the following equations:

$$\log K = \frac{-\Delta H^\circ}{2.303RT} + \frac{\Delta S^\circ}{2.303R} \quad (9)$$

$$\Delta G^\circ = \Delta H^\circ - T \Delta S^\circ \quad (10)$$

where K and R are the binding constant and gas constant, respectively. Results shown in Table 3 suggest that the process is entropically driven. The positive entropy change occurs because the water molecules that are arranged in an orderly fashion around the ligand and protein acquire a more random configuration as a result of hydrophobic interactions [44,45]. Further, specific electrostatic interactions between ionic species in aqueous solutions are characterized by a positive value of ΔS° and a negative ΔH° value (almost zero). The present ΔH° value indicates the involvement of both hydrogen bonding and electrostatic interactions. Thus, it is more likely DOX-Hb is stabilized by hydrophobic, electrostatic and hydrogen bonding forces [45].

3.7. Fourier transform infrared (FT-IR) measurements

The infrared spectra of proteins exhibit a number of amide bands, which represent different vibrations of the peptide moiety.

Table 3
Thermodynamic parameters of Hb-DOX system

T (K)	ΔG° (kJ mol $^{-1}$)	ΔH° (kJ mol $^{-1}$)	ΔS° (J mol $^{-1}$ K $^{-1}$)
298	-32.82 ± 0.05	-10.91 ± 0.07	73.53 ± 0.03
306	-33.41 ± 0.04	-10.91 ± 0.07	73.53 ± 0.03
310	-33.71 ± 0.02	-10.91 ± 0.07	73.53 ± 0.03

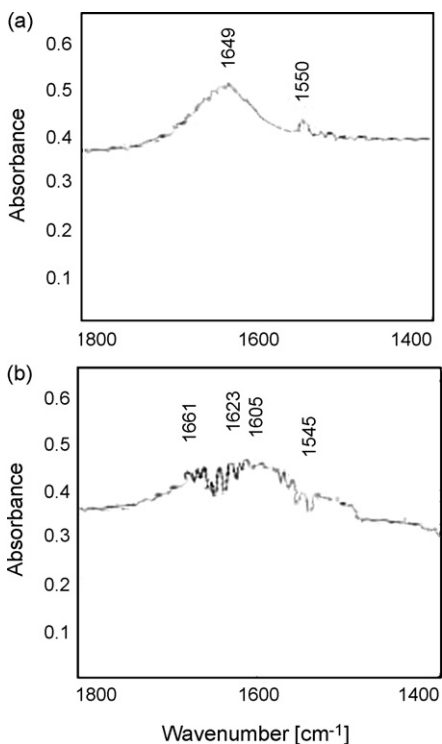


Fig. 8. FT-IR spectra of Hb and Hb-DOX complex: (a) FT-IR difference spectrum of Hb alone; (b) FT-IR difference spectrum of Hb-DOX complex; obtained by subtracting the spectrum of the DOX + buffer from that of the DOX-bound form in the region of 1800–1400 cm^{-1} at physiological pH (Hb: 3.0 μM ; ADM: 12.0 μM).

Of all the amide modes of peptide group, the single most widely used in studies of protein structure is amide I. This vibration mode originates from the C=O stretching vibration of the amide group (coupled to the in-phase bending of the N-H bond and the stretching of the C-N bond) and gives rise to infrared bands in the region between approximately 1600 and 1700 cm^{-1} [23]. This provides us information of the change occurring in protein on DOX interaction, at molecular level. Also the amide I band is most sensitive to the change of protein structure than other amide bonds [46]. Fig. 8 shows the FT-IR spectra of the DOX free and DOX-bound form of Hb with its difference absorption spectrum. The spectrum in Fig. 8a was obtained by subtracting the absorption of phosphate buffer from the spectrum of protein solution. Difference spectrum in present paper (Fig. 8b) was obtained by subtracting the spectrum of the DOX+ buffer from that of the DOX-bound form. The evident peak shift of amide I band from 1649 to 1605 cm^{-1} with its partial disappearance and appearance of new peak indicates the strong interaction of DOX with the C=O and C-N groups in the protein structural subunits. This interaction results in the rearrangement of the polypeptide carbonyl hydrogen bonding pattern and reflects reliable interaction of this drug with the peptide bonds [47]. The new absorption peak at 1623 cm^{-1} was tentatively assigned to protein aggregation or intermolecular hydrogen bonds [48,49]. So, its appearance suggests that the secondary structure of Hb has been partially destroyed and protein aggregation occurs. The distinct structural alteration is resulting in the breakage of amide bonds as suggested by the new absorption peak at 1661 cm^{-1} for reported for free C=O groups [49].

3.8. Protein degradation on Hb-DOX photoinduction

The extent of protein hydrolysis induced by the drug was estimated on the basis of the amount of acid soluble amino groups

released from the DOX treated protein. A linear increase in the absorbance of at 335 nm developed with the DOX dose range of 0–1 mM suggests substantial protein degradation, which further magnifies with increased incubation time of the reaction mixture, protein and drug (Fig. 9a). Linearity in the absorbance of acid soluble amino groups released from treated albumin suggests the dose as well as time dependent hydrolysis of protein (Fig. 9a, inset). These free amino groups could be generated upon hydrolysis of peptide bond or cleavage from α -carbon of protein [50]. The reaction was also carried out in the presence of reactive oxygen species (ROS) quenchers (mannitol and SOD). Distinct decrease in the production of acid soluble amino groups was noticed both by mannitol (8 mM) and SOD (150 U) (data not shown), which implicates the prominent role of active oxygen species in protein fragmentation and is its inhibition of free radical generation [51]. The H-abstraction by an OH^\bullet group either from peptide bond or α -carbon of amino acids and its reaction with O_2 produces peroxy species [52], which possibly on subsequent decomposition resulted in protein fragmentation. This is consistent with earlier data on protein degradation exhibiting loss of native protein fluorescence following exposure to OH^\bullet radical or combination of $\text{OH} + \text{O}_2^- (+\text{O}_2)$ [52,53]. The drug dependent diminution of protein band intensity (Fig. 9b) suggests extensive degradation of Hb.

3.9. Computational modeling of the Hb-DOX complex

Although solution experiments may more closely represent physiological conditions, it is difficult to determine the location of the binding sites. The GOLDv3.1.1 program was chosen to examine the binding mode of DOX at the active site of Hb. The best docked conformation of DOX is shown in Fig. 10. The amino acid residues involved in binding are given in Table 4. As can be seen, DOX is situated near the oxygen binding site in beta subunit of Hb,

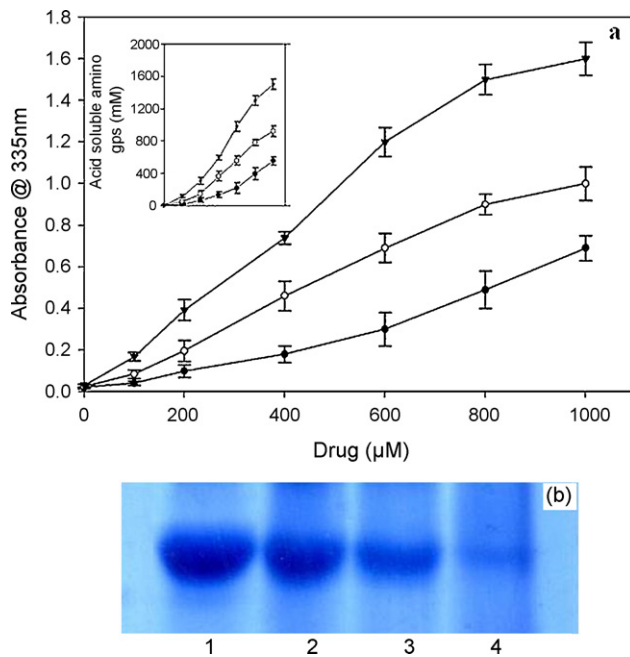


Fig. 9. Drug induced protein degradation. (a) Hb in presence of DOX at indicated concentrations was photoexcited for 2 h (●), 4 h (○) and 8 h (▼) at room temperature. The absorbance of the protein fragmentation products upon reaction with TNBS reagent was read at 335 nm. The inset shows the quantitative estimation of acid soluble amino groups released corresponding the observed absorbance. Panel (b) shows the representative SDS-PAGE of Hb when exposed to different concentration of DOX during 8 h incubation in white light. Lane 1, Hb alone; lane 2, Hb + 0.5 mM DOX; lane 3, Hb + 1.0 mM DOX; lane 4, Hb + 2.0 mM DOX.

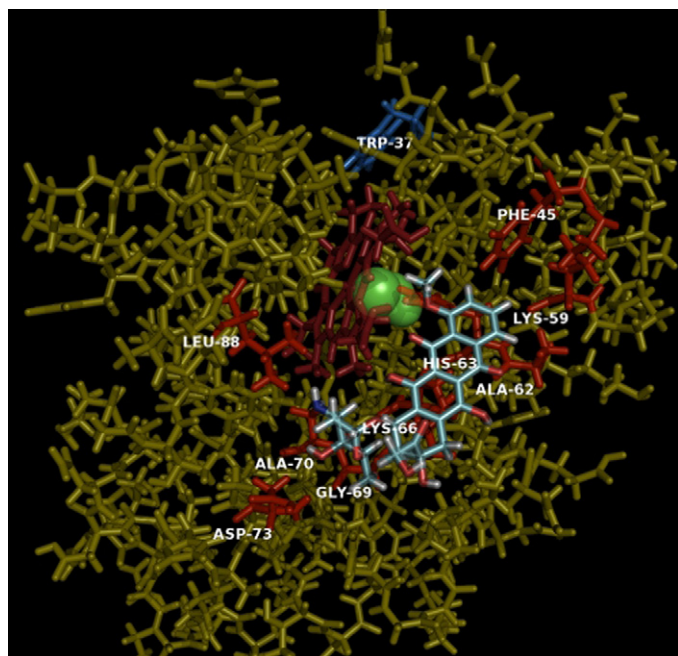


Fig. 10. Molecular modeling of DOX bound oxyHb. The ball-and-stick model represents heme ring (brown colour) and DOX molecule (cyan colour). Green colour ball near heme ring depicts bound oxygen. The residues around DOX (2 Å) has been displayed in red colour. Blue colour stick model shows the Trp 37 located at the distance 20 Å from the bound DOX. (For interpretation of the references to colour in this figure legend, the reader is referred to the web version of the article.)

where Phe45, Ala62, Ala70, Gly69 and Leu88 can make hydrophobic interactions with the phenol ring of DOX. The interaction between DOX and Hb is not exclusively hydrophobic in nature since there are several ionic as well as polar residues (His63, Asp73, Lys59, Lys66) in the proximity of the bound ligand (within 5 Å) playing important role in stabilizing DOX via H-bonds and electrostatic interactions. The hydrogen bonding or electrostatic interaction acts as an “anchor”, intensely determining the 3D space position of DOX in the binding pocket and facilitating the hydrophobic interaction of the dihydroxyanthraquinone rings with the side chain of protein. This mode of binding allows hydrogen bonding, electrostatic and hydrophobic interactions to contribute to the binding energy. It is worth mentioning that the docking procedure place ligand molecule within the vicinity of heme ring (2.37 Å) implicating its interference in the oxygen binding. Though, the interference talk may be negative or positive in reference to the oxygen transport process. It is worth mentioning that in a recent finding, the interaction of DOX with Hb induced a significant increase (22%) in oxygen affinity as compared with Hb without drug [54]. The distance calculated between the Trp 37 and the drug was found to be around

Table 4

Molecular docking analysis of the DOX binding on Hb, predicting atoms involved and estimated distances between the protein and ligand atoms

Protein atom	Ligand atom	Distance (Å)
PHE 45 CZ	37 C DOX	4.55
LYS 59 O	38 C DOX	4.57
ALA 62 O	36 C DOX	4.07
HIS 63 ND1	11 O DOX	2.68
LYS 66 CG	27 C DOX	3.12
GLY 69 CA	29 C DOX	4.38
ALA 70 CB	12 N DOX	4.16
ASP 73 OD2	04 O DOX	3.81
LEU 88 CD1	12 N DOX	3.76
HEM 1 O1A	05 O DOX	2.37

19 Å, which corroborates with the approximate distance derived by the FRET.

4. Conclusion

The results obtained gave vital yet less explored information on the binding of DOX to Hb. The spontaneous binding process is characterized by increased entropy and decreased enthalpy. The bound Hb molecules are induced to undergo secondary and tertiary conformational transitions. The thermodynamic results revealed that hydrophobic, hydrogen bonding and electrostatic interactions played a major role in stabilizing the complex. The results of synchronous fluorescence spectroscopy indicated that the environments of Trp residues were altered and the physiological state of Hb was affected by DOX. Docking calculations suggested that the best energy results favours, DOX binding at β -subunit of the protein. The binding study of DOX with Hb is of biochemical and toxicological importance. Also, this study has immense clinical importance as blood concentration of doxorubicin is reported to be 2.12 $\mu\text{g ml}^{-1}$ [55], which lies in the concentration range of this study.

Acknowledgements

We are thankful to the central instrumentation facility (CIF) of IBU and also acknowledge the CIF of Department of Chemistry, AMU. This work was supported by the CSIR sanction no. 37(1209)04 EMR II. SNK acknowledge the fellowship from CSIR, India.

References

- [1] F.W. Scheller, N. Bistolas, S.Q. Liu, M. Janchen, M. Katterle, U. Wollenberger, *Adv. Colloid Interface Sci.* 116 (2005) 111–120.
- [2] J.M. Berg, T.L. Tymoczko, L. Stryer, *Biochemistry*, fifth ed., Freeman, San Francisco, 2002, 894 pp.
- [3] A. De Swati, J. Girigoswami, *Colloid Interface Sci.* 296 (2006) 324–331.
- [4] R.T. Orr, D.D. Von Hoff, *Cancer Chemotherapy Handbook*, second ed., Appelton and Lang, Norwalk, CA, 1994, pp. 396–411.
- [5] J.H. Doroshov, G.Y. Locker, I. Iffrim, C.E. Myers, *J. Clin. Invest.* 68 (1981) 1053–1064.
- [6] B. Huang, G.L. Zou, D.L. Jin, H.C. Li, *Shanghai Sci* 35 (2003) 301–305.
- [7] J.W. Lown, S. Sim, K.C. Majumdar, R. Chang, *Biochem. Biophys. Res. Commun.* 76 (1977) 705–710.
- [8] J.R. Muindi, B.K. Sinha, L. Gianni, C.E. Myers, *FEBS Lett.* 172 (1984) 226–230.
- [9] J. Goodman, P. Hochstein, *Biophys. Res. Commun.* 7 (1977) 797–803.
- [10] K. Shinohara, K.R. Tanaka, *Hemoglobin* 4 (1980) 735–745.
- [11] C.A. Henderson, E.N. Metz, S.P. Balcerzak, A.L. Sagone, *Blood* 52 (1978) 878–885.
- [12] A.L. Sagone, *Am. J. Hematol.* 7 (1979) 97–106.
- [13] C.C. Winterbourn, J.K. French, R.F.C. Claridge, *Biochem. J.* 179 (1979) 665–673.
- [14] S. Ramanathan-Girish, M. Boroujerdi, *J. Pharm. Pharmacol.* 53 (2001) 815–821.
- [15] M. Dalmark, P. Johansen, *Mol. Pharmacol.* 22 (1982) 158–165.
- [16] C.E. Myers, L. Gianni, C.B. Simone, R. Klecker, R. Greene, *Biochemistry* 21 (1982) 1707–1713.
- [17] J.M. Gutteridge, *Biochem. Pharmacol.* 33 (1984) 1725–1728.
- [18] S.N. Khan, B. Islam, A.U. Khan, *Int. J. Integ. Biol.* 2 (2007) 102–112.
- [19] E. Karnaukhova, *Biochem. Pharmacol.* 73 (2007) 901–910.
- [20] R. Motterlini, R. Foresti, K. Vandegriff, M. Intaglietta, R.M. Winslow, *Am. J. Physiol.* 269 (1995) H648–H655.
- [21] B. Alpert, D.M. Jameson, G. Weber, *Photochem. Photobiol.* 31 (1980) 1–4.
- [22] T. Förster, O. Sinanoglu (Eds.), *Modern Quantum Chemistry*, vol. 3, Academic Press, New York, 1996, 93 pp.
- [23] A.C. Dong, P. Huang, W.S. Caughey, *Biochemistry* 29 (1990) 3303–3308.
- [24] S.L. Snyder, P.Z. Sobocinski, *Anal. Biochem.* 64 (1975) 284–288.
- [25] U.K. Laemmli, *Nature* 277 (1970) 680–685.
- [26] G. Jones, P. Willett, R.C. Glen, *J. Mol. Biol.* 245 (1995) 43–53.
- [27] CORINA, version 2.6, Molecular Networks GmbH, Computerchemie, Nögelsbachstraße 25, D-91052 Erlangen, Germany, 2000. Available from: <<http://www.mol-net.de>>.
- [28] R. Wang, L. Lai, S. Wang, *J. Comput. Aided Mol. Des.* 16 (2002) 11–26.
- [29] I.D. Kuntz, J.M. Blaney, S.J. Oatley, R. Langridge, T.E. Ferrin, *J. Mol. Biol.* 161 (1982) 269–288.
- [30] Y.H. Chen, J.T. Yang, *Biochemistry* 11 (1972) 4120–4131.
- [31] J. Shobini, A.K. Mishra, K. Sandhya, N. Chandra, *Spectrochim. Acta A* 57 (2001) 1133–1147.
- [32] J.L. Miles, E. Morey, F. Crain, S. Gross, J. San Julian, W.L. Canady, *J. Biol. Chem.* 237 (1962) 1319–1322.

- [33] J.R. Lakowicz, *Biochemistry* 12 (1973) 4161–4170.
- [34] R.E. Maurice, A.G. Camillo, *Anal. Biochem.* 114 (1981) 199–212.
- [35] Y.Q. Wang, H.M. Zhang, G.C. Zhang, S.X. Liu, Q.H. Zhou, Z.H. Fei, Z.T. Liu, *Int. J. Biol. Macromol.* 41 (2007) 243–250.
- [36] J.B.F. Lloyd, *Nat. Phys. Sci.* 231 (1971) 64–65.
- [37] J.N. Miller, *Proc. Anal. Div. Chem. Soc.* 16 (1979) 203–208.
- [38] J. Baldwin, C. Chothia, *J. Mol. Biol.* 129 (1979) 175–220.
- [39] A. Haouz, S.E. Mohsni, C. Zentz, F. Merola, B. Alpert, *Eur. J. Biochem.* 264 (1999) 250–257.
- [40] B. Valeur, J.C. Brochon, *New Trends in Fluorescence Spectroscopy*, sixth ed., Springer Press, Berlin, 1999, 25 pp.
- [41] A.E.A. Thumser, A.G. Buckland, D.C. Wilton, *J. Lipid. Res.* 39 (1998) 1033–1038.
- [42] N. Seedher, B. Singh, P. Singh, *Indian J. Pharm. Sci.* 61 (1999) 143–148.
- [43] P.D. Ross, S. Subramanian, *Biochemistry* 20 (1981) 3096–3102.
- [44] H. Aki, M. Yamamoto, *J. Pharm. Pharmacol.* 41 (1989) 674–679.
- [45] W. He, Y. Li, C. Xue, Z. Hu, X. Chen, F. Sheng, *Bioorg. Med. Chem.* 13 (2005) 1837–1845.
- [46] W.K. Surewicz, H.H. Mantsch, D. Chapman, *Biochemistry* 32 (1993) 389–394.
- [47] H.L. Casal, U. Kohler, H.H. Mantsch, *Biochim. Biophys. Acta* 957 (1988) 11–20.
- [48] J.M. Purcell, H. Susi, *J. Biochem. Biophys. Methods* 9 (1984) 193–199.
- [49] C. Liu, A. Bo, G. Cheng, X. Lin, S. Dong, *Biochim. Biophys. Acta* 1385 (1998) 53–60.
- [50] K.J. Davies, M.E. Delsignore, *J. Biol. Chem.* 262 (1987) 9908–9913.
- [51] D.A. Bates, C.C. Winterbourn, *Biochem. J.* 203 (1982) 155–160.
- [52] K.J. Davies, *J. Biol. Chem.* 262 (1987) 9895–9901.
- [53] K.J. Davies, M.E. Delsignore, S.W. Lin, *J. Biol. Chem.* 262 (1987) 9902–9907.
- [54] F. Misiti, B. Giardina, A. Mordente, M.E. Clementi, *Braz. J. Med. Biol. Res.* 36 (2003) 1643–1651.
- [55] L. Lundgren-Eriksson, A. Carlsson, S. Eksborg, W. Ryd, R. Vesanen, R. Hultborn, *Cancer Chemother. Pharmacol.* 40 (1997) 419–424.